Nanostructured Polymers Obtained from Polyethylene-*block*-poly(ethylene oxide) Block Copolymer in Unsaturated Polyester

Christophe Sinturel,*,† Marylène Vayer,† René Erre,† and Heinz Amenitsch‡

Centre de Recherche sur la Matière Divisée, 1 B rue de la Férollerie, 45071 Orléans Cedex 2, France, and Institute of Biophysics and Nanosystems Research, Austrian Academy of Sciences, Schmiedlstr. 6, 8042 Graz, Austria

Received December 13, 2006; Revised Manuscript Received January 22, 2007

ABSTRACT: We report the phase behavior, the molecular assembly, and the crystallization in blends of unsaturated polyester resin (UP, thermoset polymer) and low molecular mass polyethylene-*block*-poly(ethylene oxide) (EEO, 1400 g mol^{-1}). Liquid blends containing 2.5−25% of EEO block copolymer were prepared. At a macroscopic level, all the prepared blends are homogeneous at room temperature, exhibiting LCST-type behavior upon heating, with macrophase separation occurring at 75 °C in the studied range of compositions. Curing at a temperature lower than 75 °C prevents macrophase separation and allows the fixing of the structure obtained in the initial liquid state. In these conditions, EEO platelets exhibiting a high aspect ratio (6 nm thick, 500 nm to 1 μm long) constituted of a crystalline PE core, bordered by PEO domains, are observed in the cured state by TEM. For low EEO content, isolated lamellae are obtained. For higher content, aggregation of the lamellae is observed without real isotrope/nematic transformation. These observations are in close correspondence with the real-time SAXS−WAXS experiments that permit us to follow the molecular assembly of the block copolymer upon heating. DSC study of the blends indicates that PEO crystallization is suppressed, which confirms the miscibility of the PEO segments with the UP. Concerning PE blocks, a strong depression of the crystallization temperature is observed in the cured samples, suggesting a confinement effect.

Introduction

In the considerably wide field of polymer blends based on thermosetting polymers, nanostructured materials obtained from systems containing block copolymers have attracted a great deal of attention over the past decade.

Initiated in the late 1990s,[1] one of the most simple and popular approaches consists in forming self-organised mesophases prior to curing (lamellar, bicontinuous, cylindrical, spherical) by combining an amphiphilic block copolymer and a network-forming liquid precursor that selectively mixes the blocks of the copolymer. Further curing fixes the initial morphology and leads to solid cured materials containing nanosize heterogeneities. Using this strategy, various nanostructured materials have been prepared depending on the composition of the blends, on the block copolymer characteristics (composition, size, and relative proportion of the blocks), and on the type of thermoset precursors. Since this pioneer work, studies have mainly concerned epoxy resins and nonreactive copolymers.[2] Nanostructured polymers based on phenolic resol resin have also been reported.[3] In this approach the absence of macrophase separation upon curing is a key factor for keeping the initial self-organized mesophases and thus obtaining nanostructured materials. Nevertheless, this is not always achievable, and phase separation can be induced in the system by the unfavorable entropic contribution to the mixing free energy resulting from the increase in molecular weight of the thermoset precursor due to the cross-linking (reaction-induced phase separation, RIPS). This phenomenon can be attenuated in some cases with the use of block copolymers containing reactive chain ends that can react with the thermoset precursors.[4] In other cases, phase separation cannot be avoided, particularly when gelation (that fixes the morphology of the system) occurs at high conversion degree (like epoxy resins), allowing the molecular weight of the thermoset precursor to increase largely before gelation.

Considering this, it is surprising that the strategy of forming self-organized mesophases prior to curing has seldom been investigated for thermoset polymers[5] exhibiting a low conversion degree at gel point such as unsaturated polyester resins (UP)[6] which are in addition a very popular class of thermosetting polymers. UP indeed find a wide range of applications (automotive and electric industries, electric household appliances, etc.) thanks to easy processability, good mechanic performance and surface aspect, easy curing, etc. Composed of low molecular mass chains of unsaturated polyester (<5000 g mol^{-1}) in solution in styrene, UP are transformed into a cross-linked network by free-radical reactions with styrene. Interestingly, modification of UP by nonreactive low molecular mass polymers is already a common feature for improvement of the surface aspect and shrinkage compensation.[7] In most of the cases, homogeneous blends of UP and thermoplastic additive are used. This latter does not participate in the curing reaction but induces phase separation in the blend until gelation.[8] It has been indeed recently demonstrated that due to the low value of the conversion degree at gel point, phase separation usually interacts rapidly with the cross-linking reaction (gelation) that hinders further evolution.[9] Macroscopic phase separation can be then prevented by selecting the appropriate blends and curing conditions. Control of the separated domains size within a nanoscale can be achieved leading to the expected properties. However, the number of systems giving such results is limited.

For all these reasons, the temptation is strong to use the strategy based on block copolymer instead of this approach

* Corresponding author: e-mail christophe.sinturel@univ-orleans.fr; Tel 33-(0)238 494 737; Fax 33-(0)238 255 376.
† Centre de Recherche sur la Matière Divisée.
‡ Austrian Academy of Sciences.

10.1021/ma062849r CCC: $37.00
Published on Web 02/15/2007

based on "frustrated phase separation": the size of the dispersed features can be controlled accurately, self-organization of the additive can be achieved, and a wide variety of additives can be used (including block copolymer with crystalline segments). This can be reached by selecting block copolymers presenting different affinities toward the host resin. Low molecular mass polyethylene-*block*-poly(ethylene oxide) (EEO, 1400 g mol^{-1}) was selected: PEO is indeed known to be miscible in UP,[10] whereas PE is not. At room temperature pure EEO exhibits a self-assembled lamellar structure with crystallized domains of PE and PEO[11] which can add interesting properties to the amorphous cross-linked UP systems. The purpose of this work is to demonstrate that nanostructured materials can be obtained from unsaturated polyester resin, using the strategy introduced some years ago with epoxy.

To be totally exhaustive on the various approaches used to generate nanostructurated material from thermoset blends, one has to note that RIPS have been recently successfully employed in blends containing block copolymer.[12] In this case, curing was performed in initially miscible blends of triblock copolymers (PCL−PB−PCL) and epoxy. Nanostructures were then obtained by polymerization-induced microphase separation of the central block whereas lateral blocks remain miscible with the epoxy. In our case, PE segments are nonmiscible with the thermoset precursor whatever the temperature.

Experimental Section

Samples Preparation. The EEO diblock copolymer, namely polyethylene-*block*-poly(ethylene oxide), was purchased from Aldrich Chemical Co. It has an average M_n = 1400 g mol^{-1} and contains 50 wt % ethylene oxide. It was used without further purification. This commercial product presents a broad mass distribution and also contains homopolymer impurities. Subchains of polyethylene and poly(ethylene oxide) will be respectively designed by PE and PEO.

The uncured unsaturated polyester resin (UP) consists of unsaturated polyester prepolymer in solution in styrene. The prepolymer Palapreg P18-03 (from DSM Composite resins) is made from maleic anhydride, propylene glycol, and neopentyl glycol. Styrene amount was calculated to adjust the C═C molar ratio between styrene and prepolymer to 1. The resulting mixture is liquid at room temperature.

Lauryl peroxide (LP) purchased from Aldrich Chemical Co. was used as free radical polymerization initiator, without further purification.

To prepare the UP/EEO blend, UP (liquid) and EEO (solid) were first mixed at room temperature. At this temperature, it was observed that formation of a homogeneous system was only reached after long stirring (several days). For shorter time periods, particles of copolymer still remain in the mixture. Thus, the blends were prepared from mixtures in the molten state (120 °C). For this purpose, the components were poured into a three-necked flask equipped with a mechanical stirrer, a thermometer, and a condenser and heated to 120 °C under vigorous stirring (350 rpm) and left 15 min at this temperature. The mixture was then slowly cooled to room temperature under continuous stirring. In these conditions, homogeneous systems were also obtained. Various blends containing 2.5−25 wt % of EEO block copolymer were prepared. Higher concentrations were not considered because of the high viscosity of the blends reached at these concentrations. Initiated UP/EEO blends were prepared by adding at room temperature the free radical initiator under continuous stirring. The initiator was added in the proportion of 1 wt % of UP.

Differential Scanning Calorimetry (DSC). The calorimetric measurements were performed on a Perkin-Elmer Pyris DSC 6 differential scanning calorimeter. The instrument was calibrated with indium and dry cyclohexane standards. Dry nitrogen was used as the purge gas (20 mL min^{-1}), and samples of 15−20 mg were analyzed. Noninitiated blends were heated up to 135 °C and then cooled to −30 °C. Initiated blends were cured during isothermal step at 70 °C for 1 h. Samples were then heated to 135 °C and then cooled to −30 °C. All the ramps were carried out at 10 °C/min.

Transmission Electron Microscopy (TEM). TEM observations were performed on fully cured solid samples. Initiated liquid blends were poured in aluminum molds with the help of a spatula. Samples were then cured at 70 °C for 1 h, heated to 135 °C for postcuring at 10 °C/min, and then cooled. Obtained samples were microtomed with a diamond knife. The resulting ultrathin sections (50 nm thick) were placed on copper grids and stained in vapor of a solution of RuO_4 to optimize the contrast between the phases and to limit deformations of the microtomed samples in the electron beam. The RuO_4 staining solution was prepared using NaOCl solution and $RuCl_3$ following a procedure described in the literature by Brown and Butler.[13] TEM was performed on a Philipps CM20 where an acceleration voltage of 120 kV and a resolution of 0.7 nm were used. The electron gun was equipped with a LaB_6 monocrystal for a high brilliance.

Optical Microscopy. Morphological changes during curing were observed using an Olympus BX51 optical microscope coupled with a Linkam LTS350 heating plate, controlled by a Linkam TMS94 controller. Images were continuously recorded with a Sony Exwave HAD CCD camera interfaced with the Pinnacle Studio version 9 software. A droplet of blend was introduced between two thin glass coverslips and placed in the Linkam sample stage. The stage was then heated from room temperature to 135 °C using a heating rate of 5 °C/min.

Small-Angle X-ray Scattering (SAXS) and Wide-Angle X-ray Scattering (WAXS). Simultaneous 2D SAXS and 1D WAXS were performed at the Austrian SAXS Beamline 5.2L of the electron storage ring ELETTRA (Italy) working with incident X-rays of 8 keV.[14] The SAXS pattern was detected by a 2D image plate detector MAR180 (MarResearch, Hamburg, Germany) placed at 234 cm from the sample in the q range from 0.07 to 2 nm^{-1}. The WAXS pattern was measured with a 1D gas detector based on the delay line principle[14] in the q range from 7 to 17 nm^{-1}. The calibration of the angular scale was performed with silver behenate CH_3-$(CH_2)_{20}$−COOAg (d-spacing: 5.838 nm)[15] for the SAXS detector and with p-bromobenzoic acid[16] for the WAXS detector. Viscous UP/EEO blends were poured into quartz capillaries with 1.5 mm internal diameter. The capillaries were inserted into a custom-made DSC (MicroCalix, Physico Chimie des Systèmes Polyphasés, Paris). The calibration of the DSC was performed with lauric acid.

Results and Analysis

Characterization of the Blends Prior to Curing. At room temperature, all the UP/EEO blends are initially transparent, suggesting a homogeneous composition of the systems at the scale of the visible light wavelength. This has been confirmed by optical microscopy (OM) where plain images are observed at this scale. Upon heating (from RT to 135 °C), the noninitiated systems exhibit a macroscopic phase separation when the temperature increases. Figure 1 gives the example of a system containing 20 wt % of EEO block copolymer.

Beginning at room temperature, the system remains homogeneous up to 75 °C. At this temperature, phase separation starts to develop, leading to separated domains with a micrometer scale size. With subsequent heating, domains increase in size. In the range of the studied concentrations (2.5−25 wt %), all the systems exhibit similar behavior, with the onset of phase separation located near 75 °C. This phase behavior should be compared with the behavior of PE and PEO homopolymers in UP. PE is completely immiscible with UP. Concerning PEO, we have recently shown that PEO oligomers exhibit LCST type behavior in UP.[17] This is in agreement with other works[10]

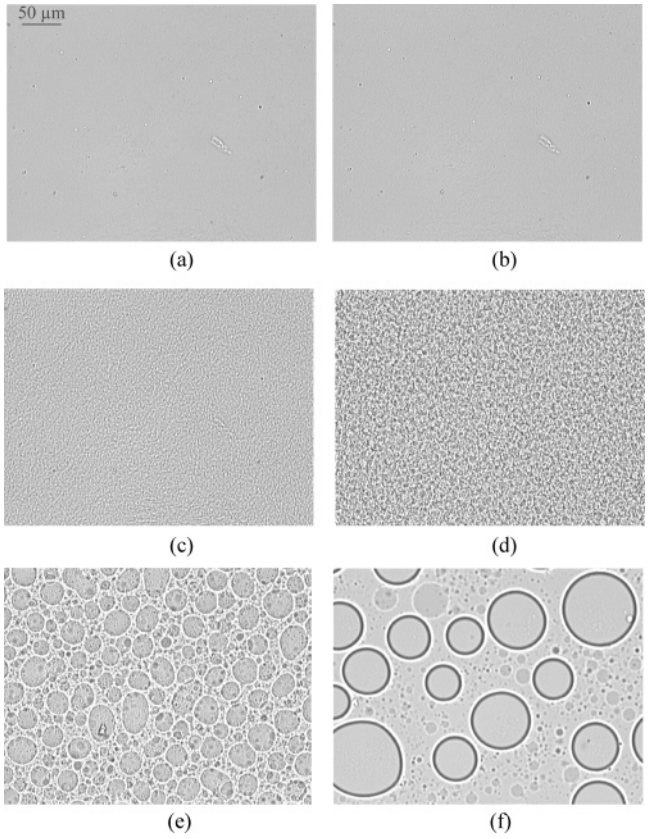

Figure 1. OM micrographs of noninitiated UP/EEO 80/20 blend at 55 (a), 70 (b), 75 (c), 85 (d), 90 (e), and 110 °C (f). All magnifications are ×200. Same scale bar for all micrographs.

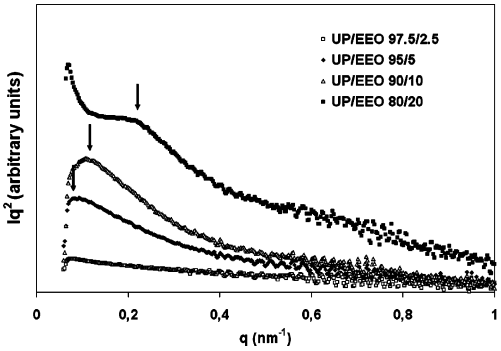

Figure 2. Initial SAXS patterns of uncured UP/EEO blends at room temperature.

demonstrating favorable interactions between PEO and UP, at moderate temperature, resulting from hydrogen bonding between the ether oxygen of the PEO and the UP chain termination which, in our conditions, can be either hydroxyl or carboxylic functions. As hydrogen bonds are thermally labile, a rise in temperature reduces the number of bonds and eventually causes phase separation. Unexpectedly, all the systems exhibit phase separation at a similar temperature upon heating whereas concentration dependence is classically obtained.

In order to assess the structure of the obtained mixtures at a nanoscopic level, SAXS was performed. Figure 2 shows the SAXS patterns of the uncured UP/EEO blends at room temperature (2.5, 5, 10, and 20%).

Prior to curing, all the systems exhibit similar behavior (except for UP/EEO 97.5/2.5) with a maximum at low q values ($0.07-0.2$ nm^{-1}), suggesting the presence of correlated domains within the nanometric scale. Table 1 gives the q value of the maximum observed for each blend with the corresponding correlation distance.

Table 1. q Value and Corresponding Correlation Distance of the Correlation Peak of the SAXS Pattern Obtained for the Uncured UP/EEO Blends Prior to Heating

EEO content (%)	q (nm^{-1})	d (nm)
5	0.07	90
10	0.10	63
20	0.20	31

This behavior was confirmed in SANS (not shown here) where similar scattering patterns were observed. These results should be compared to the SAXS results obtained on the pure EEO by Sun et al.[11] At room temperature, pure EEO exhibits a SAXS pattern with the principal reflection located at $q = 0.51$ nm^{-1} and secondary reflections at $2q$ and $3q$ which are typical hallmarks of a lamellar structure with a long period spacing of 12.3 nm. As seen above, UP/EEO blends exhibit only one maximum, suggesting that the lamellar structure is lost in the blends and replaced by correlated nanometer scale domains.

Curing: Selection of a Protocol and Characterization by in-Situ Measurements. In order to cure the system without macroscopic phase separation, cross-liking initiator exhibiting decomposition before the phase separation (75 °C) was added to the system. For this purpose, LP (half-life time of 3.5 h at 70 °C[18]) was selected. In this case, the system was set at 70 °C for 1 h (in order to reach the gelation) and subsequently heated to 135 °C (postcuring). In these conditions and whatever the EEO concentration, no macroscopic phase separation was observed by optical microscopy. It indicates that cross-linking of the liquid UP prepolymer allows gelation of the system, preventing macrophase separation.

In order to characterize the system upon curing, SAXS was performed during the thermal treatment (curing, postcuring, and cooling). Figure 3 shows the variation of the SAXS pattern for a blend containing 20 wt % of EEO upon heating (a) and cooling (b).

One can see that curing leads to a significant increase in scattered intensity at low q values when the curing temperature is reached. This behavior has been already observed in numerous scattering studies concerning UP curing and is often attributed to the scattering of the microgels formed upon curing. In the meantime, a weak scattering peak appears at 0.8 nm^{-1}. The intensity of this peak remains constant during the isothermal step (70 °C, 1 h) but increases again during the postcuring step to reach a maximum at 105 °C. Further increase of temperature does not lead to a significant modification of the scattered intensity. When the system is cooled from high temperature (Figure 3b), the intensity at 0.8 nm^{-1} decreases near 105 °C and finally vanishes at room temperature. In the meantime, the intensity at low q values also decreases. The origin of the peak at 0.8 nm^{-1} and the global evolution of the scattering pattern upon temperature are discussed below.

In order to follow the behavior of the crystalline domains, WAXS measurements were performed simultaneously with the SAXS experiments. The initial diffraction pattern clearly exhibits the intense PE(110) diffraction peak at 15.2 nm^{-1}. Other reflections are weaker and will not be considered here. Particularly, PEO reflections are not observed, which is in good agreement with the miscibility of PEO in UP. Upon heating, the PE(110) diffraction peak gradually decreases from 70 °C and vanishes at 105 °C, corresponding to the gradual melting of the PE domains. Symmetrical behavior is obtained upon cooling with a gradual increase of the diffraction peak at 15.2 nm^{-1}, corresponding to the crystallization of the PE domains.

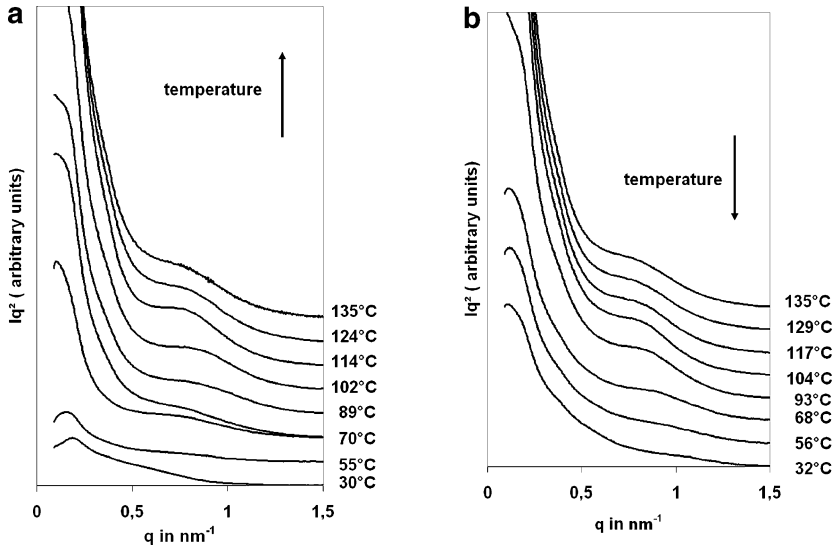

Figure 3. (a) Temperature dependence of the SAXS profile of initiated UP/EEO 80/20 blend upon heating from RT to 70 °C at 5 °C/min, curing for 60 min at 70 °C, and heating up to 135 °C at 5 °C/min. (b) Temperature dependence of the SAXS profile of cured UP/EEO 80/20 blend upon cooling from 135 °C to RT at 5 °C/min.

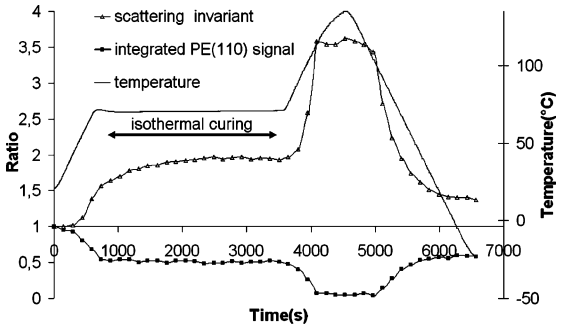

Figure 4. Evolution of the SAXS partial invariant and the PE(110) integrated intensity (ratio over the initial value) for LP initiated UP/EEO 80/20 blend upon heating from RT to 70 °C, curing during 60 min at 70 °C, heating from 70 °C up to 135 °C, and cooling down at 5 °C/min.

SAXS and WAXS data variations can be interestingly compared by plotting the integrated scattering intensity of the SAXS profile and the integrated intensity of the PE(110) diffraction peak of the WAXS pattern vs the temperature (Figure 4). The integrated scattering intensity (scattering invariant) is a measure of the total small-angle scattering from a material and can be calculated as follows:

$$Q = \frac{1}{2\pi i_e} \int_0^\infty I(q) q^2 \, dq$$

where i_e is the Thompson scattering factor. A strong correlation can be observed between the PE melting (crystallization), and the increase (decrease) of the scattered intensity in SAXS and will be discussed below.

TEM Characterization of Cured Blends. Microstructures of the fully cured system were examined by TEM (Figures 5−7). The micrographs obtained display nanoscale heterogeneities that can be interpreted as lamellae spread in a continuous matrix. For low concentrations of EEO block copolymer, the dispersion is homogeneous and the lamellae orientation is isotropic. This can be seen in Figure 5a for the sample containing 5% of EEO diblock copolymer, where various types of lamellae cross section appear, resulting from different lamellae orientations in the system. In some cases, the lamellae normal is within the plane of the cut, and the cross section of the lamellae appears white

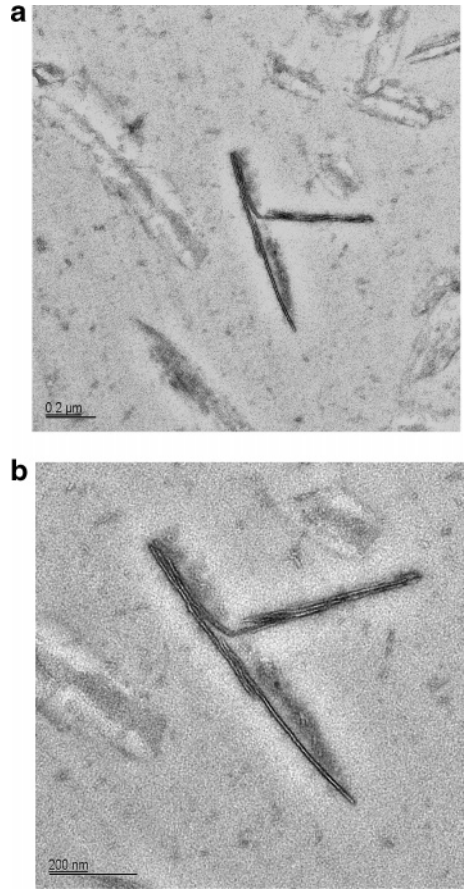

Figure 5. TEM micrograph of LP-cured UP/EEO 95/5 blend at various magnifications: (a) ×11 500 and (b) ×20 000.

in the middle whereas each side is stained in black (see Figure 5b). As PEO block is preferentially stained with RuO_4 (compared to PE block and UP), it can be concluded from the micrographs that the lamellae are composed of PE in the center while PEO is in contact with the matrix. These observations are consistent with the miscibility of PE and PEO segments with UP as discussed above. Dispersion of the immiscible PE domains is obtained by means of the PEO segments. Characteristic dimensions of the lamellae were estimated from the TEM

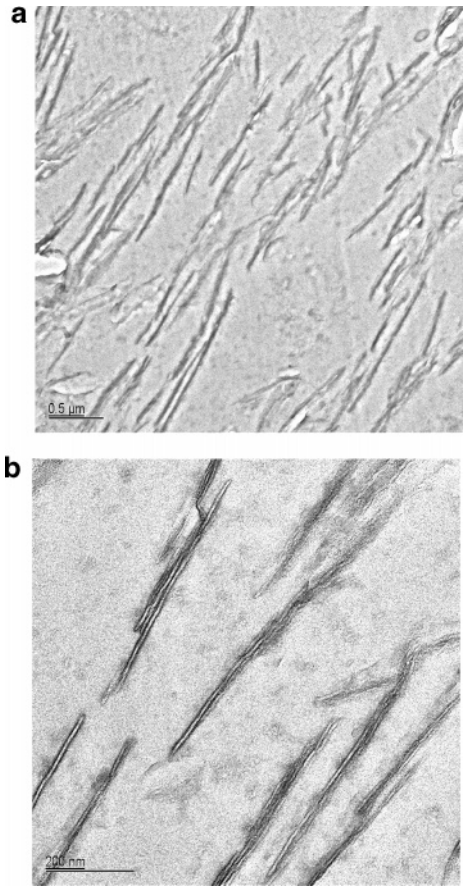

Figure 6. TEM micrograph of LP-cured UP/EEO 90/10 blend at various magnifications: (a) ×5000 and (b) ×20 000.

micrographs at high magnification. Lamellae exhibit a high aspect ratio with a thickness around 6 nm (PE domains ranging from 3 to 4 nm, PEO domains from 2 to 3 nm), whereas the length of the lamellae ranges from 500 nm to 1 μm. With increased concentration of EEO, domains with preferential orientation of the lamellae were observed. An example is shown in Figure 6a for a sample containing 10% copolymer. This behavior is consistent with the high aspect ratio of the lamellae which induces steric hindrance, leading to quasi-parallel orientation of the lamellae along a preferential axis when the concentration increases. However, the whole system remains isotropic since the orientation axis was not constant within the whole sample. From this concentration, some aggregations of the lamellae begin to be observed (Figure 6b). As the concentration increases, such behavior becomes predominant and individual lamellae are no longer observed (Figure 7).

Crystallinity Studied by DSC. As symmetrical behaviors appear for the melting and crystallization, for brevity we will herein focus only on the crystallization. Figure 8 and Figure 9 present the DSC records for UP/EEO blends containing various amounts of diblock, in the case of noninitiated and initiated samples. The DSC trace of the pure diblock is also indicated. In order to be easily compared, the curves are normalized to the same copolymer content. All these curves were recorded upon cooling from 135 °C.

For the pure diblock, a first exothermic peak at 95 °C with a shoulder at 85 °C and a second sharp exothermic peak at 15 °C are seen and attributed to the sequential crystallization of PE and PEO blocks.[11] A double crystallization peak for the PE domains can be attributed to different crystallization mechanisms (heterogeneous and homogeneous nucleation) as-

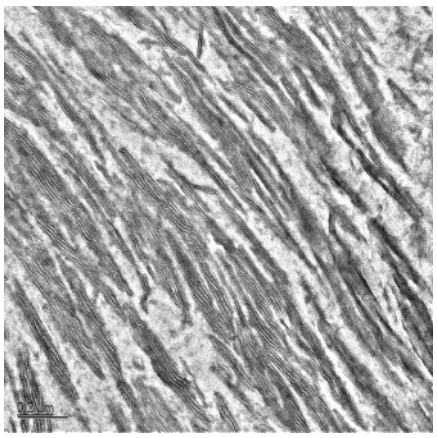

Figure 7. TEM micrograph of cured UP/EEO 75/25 blend (×11 500).

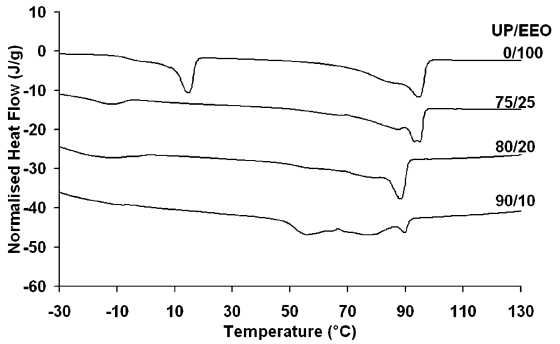

Figure 8. Normalized DSC thermograms of noninitiated UP/EEO blends obtained during cooling at 10 °C/min from 135 °C.

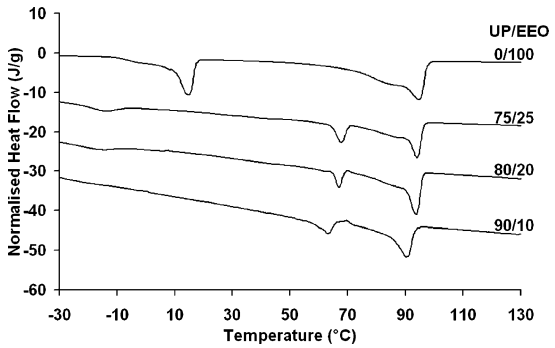

Figure 9. Normalized DSC thermograms of LP-initiated UP/EEO blends previously cured for 1 h at 70 °C, obtained during cooling at 10 °C/min from 135 °C.

sociated with a rather broad mass distribution of this commercial sample. The heat of crystallization for the PE and PEO crystals were found to be −103.9 and −45.4 J g^{-1}, respectively (or −204.8 and −90.8 J g^{-1} after normalization to the PEO and PE weight fractions). These results are lower than the values reported in previous work for fractionated samples,[11] where narrower mass distribution and elimination of homopolymer contaminants were achieved, leading to a higher extent of crystallinity.

Adding the diblock copolymer in the UP leads to significant changes in the crystallinity of the PE and PEO domains. Let us first consider the noninitiated blends (Figure 8). The major change concerns crystallization of PEO blocks. No crystallization peak can be observed for blends containing 10% or less EEO block copolymer, confirming that the PEO blocks and polyester resin are totally miscible at low temperature. For blends containing more than 10%, a small exothermic peak due

Table 2. Heat of Crystallization (J g^{-1}) of PE and PEO Domains for the Noninitiated (NI) and Cured (C) UP/EEO Blends (Measured, Calculated, and Ratio of the Two Values)

	PEO domains			PE domains		
UP/EEO	measd	calcd	ratio (%)	measd	calcd	ratio (%)
95/5 NI	0	−2.3	0	−4.9	−5.2	94
90/10 NI	0	−4.5	0	−9.3	−10.4	89
80/20 NI	−2.5	−9.1	28	−21.0	−20.8	100
75/25 NI	−3.0	−11.4	26	−23.8	−26.0	92
95/5 C	0	−2.3	0	−1.8	−5.2	35
90/10 C	0	−4.5	0	−6.0	−10.4	58
80/20 C	−1.5	−9.1	16	−15.5	−20.8	75
75/25 C	−2.1	−11.4	18	−20.2	−26.0	77

to PEO crystallization is observed, with a maximum shifted to lower temperatures ($T_{cPEO} = -10$ °C) compared to the signal of the pure block copolymer. Concerning the PE blocks, crystallization peaks have the same overall shape as the pure block copolymer with a wide exothermic peak exhibiting a maximum at 90−95 °C. For 10%, it can be observed that PE block crystallization occurs over a larger range of temperature. For each blend, the heats of crystallization of the PE and PEO domains have been calculated from the area under the exothermic peaks and compared to the expected values calculated from the content of EEO and the heat of crystallization of the pure diblocks determined previously (Table 2). As is clearly seen in this table, the blending seriously restricts the crystallization of the PEO blocks, whereas it very slightly affects the crystallization of the PE.

When the system is cured at 70 °C for 1 h prior to being heated to 135 °C, the crystallization of the PE domains exhibits two peaks (Figure 9) whatever the composition of the blends. The first one remains located at the position observed in the pure block copolymer (maximum at 95 °C, shoulder at 80 °C), whereas the second one is shifted at lower temperature (65−70 °C). The corresponding heats of crystallization, estimated by taking into account the global area under the curves of these two peaks (Table 2), show that crystallization of PE is now seriously restricted. Concerning PEO, crystallization is inhibited up to 10% of copolymer and seriously restricted for a higher content. Crystallization of the PEO domains occurs in this later case at −10 °C, which is about 25 °C lower than the temperature observed in the pure copolymer.

Discussion

The experimental procedure of the blends' preparation can be discussed. As described in the Experimental Section, we observed that the blends could be readily prepared by mixing all the components at 120 °C, followed by a cooling to room temperature under vigorous stirring. From the experimental observation, it can be stated that the mixtures first reach the two-phase state of the phase diagram, with the copolymer in the molten state (120 °C). During the second step, the cooling induces the self-organization of the block copolymer, with crystallization of the PE blocks, while in the meantime the miscibility of the PEO with the UP increases. This simultaneous behavior associated with a vigorous stirring leads to the dispersion of individual self-organized nanoplatelets constituted of a crystallized PE core bordered by PEO segments. It finally forms a homogeneous mixture (from a macroscopic point of view) containing nanometer size objects homogeneously dispersed, with isotropic orientation. This has been confirmed by SAXS results, indicating that the lamellar structure is lost in the mixture and replaced by correlated domains. The same kind of system can also be obtained by direct exfoliation of the initial layered structure of the EEO copolymer in the UP resin at room temperature but requires, on the other hand, much longer time. If we now consider the phase behavior upon heating of the noninitiated blends obtained with such a protocol, we have demonstrated that the blends exhibit a phase separation above a critical temperature which is, again, consistent with the miscibility properties of the PEO segment in UP resin. However, as PEO is here covalently bonded to the crystalline PE domain, diffusion of the PEO segment will be hindered. This can explain why all the systems exhibit phase separation at a macroscopic level at a similar temperature (75 °C) whereas concentration dependence was expected. This peculiar phase behavior, which can be tentatively related to the beginning of the PE melting, introducing mobility in the system, is still under investigation.

When the prepared systems are cured in the one-phase region of the phase diagram ($T < 75$ °C), TEM demonstrated that the initially formed nanostructures are trapped in the cross-linked network, leading to individual platelets constituted of a crystalline PE core, bordered on both sides by PEO domains. In-situ SAXS experiments performed upon curing are in good agreement with these results. It first confirms the absence of aggregation of the platelets in a periodic lattice. Only a weak single scattering peak at 0.8 nm^{-1} is indeed observed and can be attributed to the correlation of the PEO domains, separated by the PE nucleus, in the same lamella. It is interesting to note the temperature dependence of the intensity of this peak, suggesting a variation of the electronic contrast in the system with the temperature. This can be attributed to the change in specific volume associated with the melting/crystallization of PE, leading to a proportional change in electronic density of the PE domains (20%[18]) and in some cases to a drastic change in electronic contrast.[19] The strong correlation between the integrated scattering intensity of the SAXS profile and the integrated intensity of the PE(110) diffraction peak confirms this assessment. Higher contrast between PE and PEO is thus obtained when PE is in the molten state. In contrast, the absence of scattering at lower temperature suggests that the electronic densities of the PE and PEO domains are matched. This behavior will also affect the scattering at low q values, which is attributed to the correlation of the lamellae and will contribute to increase the integrated scattering intensity of the SAXS profile when PE is in the molten state.

Interestingly, we have to note that these lamellar structures were not observed in the work done by Guo et al.[20] studying the behavior of the same block copolymer (EEO, $M_n = 1400$ g mol^{-1}, 50 wt % ethylene oxide) in epoxy. Despite the similar behavior of the subchains in the host resin (epoxy selectively mixes the PEO segments whereas PE blocks are immiscible), the change in thermoset precursor but also the change in curing conditions (102 °C for 8 h) lead in their case to individual spherical core (crystalline PE)/shell (PEO) micelles (within a similar range of compositions). In our case, cross-linking is performed while PE domains are still crystalline, leading to lamellar shape structure. We check that curing at higher temperature (90 °C) does not lead to dispersed structures.

As demonstrated by DSC, the crystallization of the PE domains is maintained in the cross-linked network but occurs partially at a lower temperature. It is important to point out that this shift in crystallization temperature is induced by the cross-linking of the platelets environment since this was not observed for the uncured system. Moreover, the crystallization of the PE domains occurs within a vitrified environment since T_g of the cured UP is around 145 °C. This is known to greatly influence the crystallization behavior.[21] In a very similar system (same block copolymer in epoxy) crystallization temperature depres-

sion has been observed by Guo et al.[20] and attributed to homogeneous controlled crystallization within a confined environment. Despite different final morphologies (as recalled above), a similar interpretation is given here. However, crystallization of the PE domains remains in our case partially unchanged, indicating a partial confinement effect. We verified that this behavior was not related to the presence of PE homopolymer contamination by preparing a blend from purified EEO copolymer by fractionation in toluene, where same behavior was observed. The origin of this phenomenon is then not yet fully understood and is currently under careful examination.

Conclusion

We demonstrated that nanostructured polymers can be prepared starting from self-organized block copolymers in solution in unsaturated polyester, followed by a curing step to fix the mesophases. This strategy, widely used in the case of epoxy resin, is here reported for unsaturated polyester-based thermoset. Low molecular mass polyethylene-*block*-polyethylene oxide (1400 g mol^{-1}) was selected for that purpose: PEO is indeed known to be miscible in UP whereas PE is not. LCST-type behavior was found for all the blends with macroscopic phase separation occurring for temperature higher than 75 °C. Sample preparation consists in blending the components at the molten state (T > 120 °C) followed by a slow cooling upon vigorous mixing toward the room temperature in order to reach the one-phase region of the phase diagram. Curing was secondly performed at T < 75 °C to prevent macrophase separation. In these conditions, TEM and SAXS experiments indicated unusual final morphology, with nanostructures consisting of EEO platelets exhibiting high aspect ratio (6 nm thick, 500 nm to 1 μm long). DSC study indicates that PE domains were crystalline, which makes this kind of block copolymer a good candidate for unsaturated polyester modifiers. Introduction of dispersed crystalline nanodomains with high aspect ratio could indeed improve considerably the mechanical properties of the amorphous matrix of cross-linked unsaturated polyester. Besides this practical interest, partial confinement effect of the PE domains has been detected, making these systems interesting candidates to study the crystallization within nanoscale confined environments.

Acknowledgment. The financial support from the European Community (funding ELETTRA synchrotron experiments) is greatly acknowledged. We thank Marjorie Roulet, Hans Milongo, and Fabien Venon for their contribution in the sample preparation; Thomas Cacciaguerra, Fabienne Warmont, and Dominique Jalabert for the TEM experiments; and Menzolit for providing UP.

References and Notes

(1) (a) Hillmyer, M.; Lipic, P.; Hajduk, D.; Almdal, K.; Bates, F. *J. Am. Chem. Soc.* **1997**, *119*, 2749. (b) Lipic, P.; Bates, F.; Hillmyer, A. *J. Am. Chem. Soc.* **1998**, *120*, 8963.

(2) (a) Guo, Q.; Figueiredo, P.; Thomann, R.; Gronski, W. *Polymer* **2001**, *42*, 10101. (b) Guo, Q.; Thomann, R.; Gronski, W.; Thurn-Albrecht, T. *Macromolecules* **2002**, *35*, 3133. (c) Mijovic, J. S.; Shen, M.; Sy, J. W.; Mondragon, I. *Macromolecules* **2000**, *33*, 5235. (d) Ritzenthaler, S.; Court, F.; David, L.; Girard-Reydet, E.; Leibler, L.; Pascault, J. P. *Macromolecules* **2002**, *35*, 6245. (e) Ritzenthaler, S.; Court, F.; Girard-Reydet, E.; Leibler, L.; Pascault, J. P. *Macromolecules* **2003**, *36*, 118. (f) Wu, J.; Thio, Y. S.; Bates, F. S. *J. Polym. Sci., Part B: Polym. Phys.* **2005**, *43*, 1950.

(3) (a) Kosonen, H.; Ruokolainen, J.; Nyholm, P.; Ikkala, O. *Macromolecules* **2001**, *34*, 3046. (b) Kosonen, H.; Ruokolainen, J.; Nyholm, P.; Ikkala, O. *Polymer* **2001**, *42*, 9481. (c) Kosonen, H.; Ruokolainen, J.; Torkkeli, M.; Serimaa, R.; Nyholm, P.; Ikkala, O. *Macromol. Chem. Phys.* **2002**, *203*, 388.

(4) (a) Dean, J. M.; Grubbs, R. B.; Saad, W.; Cook, R. F.; Bates, F. S. *J. Polym. Sci., Part B: Polym. Phys.* **2003**, *41*, 2444. (b) Dean, J. M.; Verghese, N. E.; Pham, H. Q.; Bates, F. S. *Macromolecules* **2003**, *36*, 9267. (c) Grubbs, R B.; Dean, J. M.; Broz, M. E.; Bates, F. S. *Macromolecules* **2000**, *33*, 9522. (d) Guo, Q.; Dean, J. M.; Grubbs, R. B.; Bates, F. S. *J. Polym. Sci., Part B: Polym. Phys.* **2003**, *41*, 1994. (e) Rebizant, V.; Abetz, V.; Tournihac, T.; Court, F.; Leibler, L. *Macromolecules* **2003**, *36*, 9889. (f) Rebizant, V.; Venet, A. S.; Tournillhac, F.; Girard-Reydet, E.; Navarro, C.; Pascault, J. P.; Leibler, L. *Macromolecules* **2004**, *37*, 8017.

(5) Patent, WO 2006/052728 A1.

(6) (a) de la Caba, K.; Guerro, P.; Eceiza, A.; Mondragon, I. *Polymer* **1996**, *37*, 275. (b) Hsu, C. P.; Lee, L. J. *Polymer* **1993**, *34*, 4516.

(7) (a) Huang, Y. J.; Su, C. *J. Appl. Polym. Sci.* **1995**, *55*, 323. (b) Boyard, N.; Sinturel, C.; Vayer, M.; Erre, R.; Levitz, P. *Polymer* **2005**, *46*, 661. (c) Bucknall, C. B.; Davies, P.; Partridge, I. K. *Polymer* **1985**, *26*, 109. (d) Huang, Y. J.; Jiang, W. C. *Polymer* **1998**, *39*, 6631. (e) Suspene, L.; Gerard, J. F.; Pascault, J. P. *Polym. Eng. Sci.* **1990**, *30*, 1585.

(8) (a) Li, W.; Lee, L. J. *Polymer* **2000**, *41*, 685. (b) Li, W.; Lee, L. J. *Polymer* **2000**, *41*, 697.

(9) Boyard, N.; Sinturel, C.; Vayer, M.; Seifert, S.; Erre, R. *Eur. Polym. J.* **2005**, *41*, 1333.

(10) (a) Zheng, H.; Zheng, S.; Guo, Q. *J. Polym. Sci., Part A* **1997**, *35*, 3161. (b) Zheng, H.; Zheng, S.; Guo, Q. *J. Polym. Sci., Part A* **1997**, *35*, 3169.

(11) Sun, L.; Liu, Y.; Zhu, L.; Hsiao, B. S.; Avila-Orta, C. A. *Polymer* **2004**, *45*, 8181.

(12) Meng, F.; Zheng, S.; Zhang, W.; Li, H.; Liang, Q. *Macromolecules* **2006**, *39*, 711.

(13) Brown, G. M.; Butler, J. H. *Polymer* **1997**, *38*, 3937.

(14) Amenitsch, H.; Bernstorff, S.; Kriechbaum, M.; Lombardo, D.; Mio, H.; Rappolt, M.; Laggner, P. *J. Appl. Crystallogr.* **1997**, *30*, 872.

(15) Huang, T. C.; Toraya, H.; Blanton, T. N.; Wu, Y. *J. Appl. Crystallogr.* **1993**, *26*, 180.

(16) Ohura, K.; Kashino, S.; Haisa, M. *J. Bull. Chem. Soc. Jpn.* **1972**, *45*, 2651.

(17) Boyard, N.; Sinturel, C.; Vayer, M.; Erre, R. *J. Appl. Polym. Sci.* **2006**, *102*, 149.

(18) Brandrup, J.; Immergut, E. H.; Grulke, E. A. In *Polymer Handbook*, 4th ed.; John Wiley & Sons: New York, 1999.

(19) Hamley, I. W. *The Physics of Block Copolymers*; Oxford University Press: Oxford, 1998.

(20) Guo, Q.; Thomann, R.; Gronsski, W.; Staneva, R.; Ivanova, R.; Stühn, B. *Macromolecules* **2003**, *36*, 3635.

(21) (a) Chung, T.-M.; Ho, R.-M.; Kuo, J.-C.; Tsai, J. C.; Hsiao, B. S.; Sics, I. *Macromolecules* **2006**, *39*, 2739. (b) Hamley, I. W.; Fairclough, J. P. A.; Terrill, N. J.; Ryan, A. J.; Lipic, P. M.; Bates, F. S.; Towns-Andrews, E. *Macromolecules* **1996**, *29*, 8835.

MA062849R